2017

Modification of LSF-YSZ Composite Cathodes by Atomic Layer Deposition

M. Rahmanipour
University of Pennsylvania

Yuan Cheng
University of Pennsylvania

Tzia M. Onn
University of Pennsylvania

A. Donazzi
Dipartamento di Energia, Milano

John M. Vohs
University of Pennsylvania, vohs@seas.upenn.edu

See next page for additional authors

Recommended Citation

Rahmanipour, M., Cheng, Y., Onn, T. M., Donazzi, A., Vohs, J. M., & Gorte, R. J. (2017). Modification of LSF-YSZ Composite Cathodes by Atomic Layer Deposition. *Journal of the Electrochemical Society, 164* F879-F884. http://dx.doi.org/10.1149/2.0181709jes

Modification of LSF-YSZ Composite Cathodes by Atomic Layer Deposition

Abstract

composite, Solid-Oxide-Fuel-Cell (SOFC) electrodes of $La_{0.8}Sr_{0.2}FeO_3$ (LSF) and yttria-stabilized zirconia (YSZ) were prepared by infiltration methods and then modified by Atomic Layer Deposition (ALD) of ZrO_2, La_2O_3, Fe_2O_3, or La_2O_3-Fe_2O_3 codeposited films of different thicknesses to determine the effect of surface composition on cathode performance. Film growth rates for ALD performed using vacuum procedures at 573 K for Fe_2O_3 and 523 K for ZrO_2 and La_2O_3 were determined to be 0.024 nm ZrO_2/cycle, 0.019 nm La_2O_3/cycle, and 0.018 nm Fe_2O_3/cycle. For ZrO_2 and Fe_2O_3, impedance spectra on symmetric cells at 873 K indicated that polarization resistances increased with coverage in a manner suggesting simple blocking of O_2 adsorption sites. With La_2O_3, the polarization resistance decreased with small numbers of ALD cycles before again increasing at higher coverages. When La_2O_3 and Fe_2O_3 were co-deposited, the polarization resistances remained low at high film coverages, implying that O_2 adsorption sites were formed on the co-deposited films. The implications fo these results for future SOFC electrode development are discussed.

Keywords

Atomic Layer Deposition, EIS, Lanthanum Ferrate, performance, SOFC cathode, solid oxide fuel cell, YSZ

Disciplines

Biochemical and Biomolecular Engineering | Chemical Engineering | Energy Systems | Engineering

Author(s)

M. Rahmanipour, Yuan Cheng, Tzia M. Onn, A. Donazzi, John M. Vohs, and Raymond J. Gorte

Modification of LSF-YSZ Composite Cathodes by Atomic Layer Deposition

M. Rahmanipour,[a,b,=] Y. Cheng,[a,=] T. M. Onn,[a] A. Donazzi,[b,*] J. M. Vohs,[a,*] and R. J. Gorte[a,,z]**

[a]*Department of Chemical and Biomolecular Engineering, University of Pennsylvania, Philadelphia, Pennsylvania 19104, USA*
[b]*Dipartimento di Energia, Politecnico di Milano, 20156 Milano, Italy*

Composite, Solid-Oxide-Fuel-Cell (SOFC) electrodes of $La_{0.8}Sr_{0.2}FeO_3$ (LSF) and yttria-stabilized zirconia (YSZ) were prepared by infiltration methods and then modified by Atomic Layer Deposition (ALD) of ZrO_2, La_2O_3, Fe_2O_3, or La_2O_3-Fe_2O_3 codeposited films of different thicknesses to determine the effect of surface composition on cathode performance. Film growth rates for ALD performed using vacuum procedures at 573 K for Fe_2O_3 and 523 K for ZrO_2 and La_2O_3 were determined to be 0.024 nm ZrO_2/cycle, 0.019 nm La_2O_3/cycle, and 0.018 nm Fe_2O_3/cycle. For ZrO_2 and Fe_2O_3, impedance spectra on symmetric cells at 873 K indicated that polarization resistances increased with coverage in a manner suggesting simple blocking of O_2 adsorption sites. With La_2O_3, the polarization resistance decreased with small numbers of ALD cycles before again increasing at higher coverages. When La_2O_3 and Fe_2O_3 were co-deposited, the polarization resistances remained low at high film coverages, implying that O_2 adsorption sites were formed on the co-deposited films. The implications of these results for future SOFC electrode development are discussed.
 [DOI: 10.1149/2.0181709jes]

Manuscript submitted April 19, 2017; revised manuscript received June 7, 2017. Published June 14, 2017.

Atomic Layer Deposition (ALD) is attracting an increasing level of attention as a method for modifying SOFC electrodes because the surface composition can be modified with unparalleled precision.[1–11] Uniform, atomic-scale films are formed in ALD by repeated cycles in which the surface is first allowed to react with an organometallic precursor, followed by a subsequent oxidation step. Since the reaction of the precursor with the surface is performed under conditions which limit the extent of reaction to one monolayer at most, the thickness of the final oxide film can be precisely controlled by the number of cycles.

In the case of SOFC cathodes, ALD has been used to improve both electrode stability and decrease impedance.[1–4] For example, Gong et al. reported that degradation rates for cathodes based on $La_{0.6}Sr_{0.4}Co_{0.2}Fe_{0.8}O_{3-\delta}$ (LSCF) decreased significantly after depositing a 5-nm ZrO_2 film.[3,4] While they reported a slight increase in the initial electrode impedance, the performance of the ALD-modified electrode surpassed that of the unmodified electrode after less than 100 h and exhibited a much lower impedance after 900 h of operation at 1073 K. In another example of cathodes modified by ZrO_2 ALD films, the initial impedance of composite cathodes of Sr-doped $LaMnO_3$ (LSM) and yttria-stabilized zirconia (YSZ) actually decreased following deposition of films as thick as 60 nm.[5]

However, studies in which electrodes were modified by ALD with other oxides have shown deleterious effects on performance. Yu et al. examined submonolayer coverages of CeO_2, SrO, and Al_2O_3 on Sr-doped $LaFeO_3$ (LSF) cathodes and reported that each of these blocked sites for oxygen adsorption.[12] Likewise, Choi et al. found that addition of CoO_x layers onto $La_{0.6}Sr_{0.4}CoO_3$ (LSC) cathodes increased electrode polarization by reducing the oxygen-exchange reaction.[6] This latter study is particularly revealing because it had been previously reported that infiltration of CoO_x nanoparticles could be used to decrease cathode polarization.[13] Choi et al. suggested that addition of CoO_x by ALD differs from infiltration because infiltration produces inhomogeneous layers that affect surface area and because the infiltration process may induce changes in the cathode morphology.[6] In principle, ALD allows catalytic materials to be added to the electrode surface as homogeneous layers, without changing the electrode morphology.

The properties of films prepared by ALD appear to depend on the specific deposition conditions that are used, especially when ALD is performed on porous materials. In the above examples of ZrO_2 films on SOFC cathode materials, the growth rates using tetrakis (dimethylamino)-zirconium (TDMZ) as the precursor were reported to be 0.57 nm/cycle[5] and 0.67 nm/cycle[4] at 583 and 573 K, respectively. In both cases, the ZrO_2 films were uniform throughout the porous electrodes but were themselves porous. Using the same precursor, Onn et al. reported ZrO_2 films deposited onto high-surface-area alumina formed dense, conformal films with a growth rate of 0.02 nm/cycle.[14] Finally, Keuter et al. reported formation of dense ZrO_2 films on SOFC anode materials, with a growth rate of 0.1 nm/cycle, using a chemically similar precursor, tetrakis (ethylmethylamino)-zirconium.[1] Major differences in the procedures used in these studies are the deposition temperatures and whether or not the substrates were exposed to the precursor in the presence of an inert carrier gas.

In the present work, we have investigated the effect of modifying an LSF-YSZ electrode with dense films of ZrO_2, La_2O_3, Fe_2O_3, and $LaFeO_3$, all formed by ALD. While each of the pure oxides appear to block O_2 adsorption sites on the cathode, we show evidence that co-deposited La_2O_3-Fe_2O_3 films could form O_2 adsorption sites on the SOFC cathode.

Experimental

ALD was performed in a homebuilt system that has been described in detail in other publications.[12,15–17] The system is essentially an adsorption apparatus that can be evacuated with a mechanical pump to approximately 10^{-3} torr. The system consists of separate chambers for the substrate and two precursors, separated by high-temperature valves. Separate furnaces were placed around each chamber, as well as around the lines between the chambers, in order to control the temperature in each section. The evacuated sample could be exposed to one of the precursor molecules by simply allowing the vapor from the precursor chamber to flow into the sample chamber. Diffusion limitations in the porous samples were minimized by not having an inert carrier gas included with the precursor. After evacuation, the sample could then be oxidized by exposure to water vapor or O_2. The precursors used in the present study were tetrakis (2,2,6,6-tetramethyl-3,5-heptanedionato) zirconium ($Zr(TMHD)_4$, Strem Chemical, Inc.), tris(2,2,6,6-tetramethyl-3,5-heptanedionato) lanthanum ($La(TMHD)_3$, Strem Chemical, Inc.), and ferrocene ($Fe(Cp)_2$, Sigma Aldrich). The deposition temperatures were chosen to be 573 K for Fe_2O_3 and 523 K for ZrO_2 and La_2O_3.

=These authors contributed equally to this work.
*Electrochemical Society Member.
**Electrochemical Society Fellow.
zE-mail: gorte@seas.upenn.edu

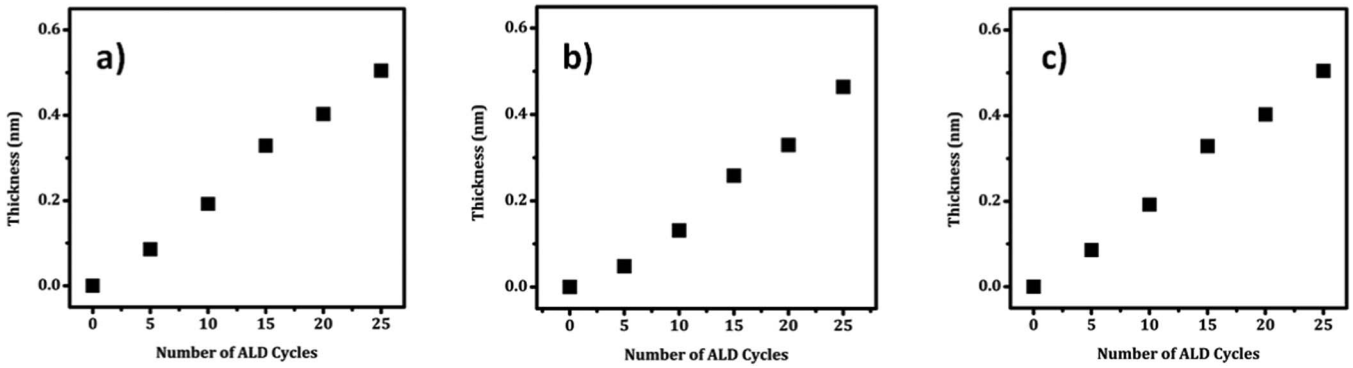

Figure 1. Growth rate as a function of number of ALD cycles on γ-Al_2O_3 for a) ZrO_2, b) La_2O_3 and c) Fe_2O_3.

Because the ligands for the La and Zr precursors could not be oxidized with O_2 or water at the deposition temperature, the samples used in this study were removed from the system and oxidized in a muffle furnace at 773 K for 5 min after each deposition cycle. Later studies showed that the ligands could be effectively oxidized at the deposition temperature using NO_2 as the oxidant and that identical growth rates for ZrO_2 on γ-Al_2O_3 could be achieved by sequential dosing of the $Zr(TMHD)_4$, precursor and NO_2. As discussed in previous papers,[15,16] varying the exposure times and pressures did not affect deposition rates for the conditions used in these experiments.

An attempt to observe changes in the sample by Scanning Electron Microscopy (SEM) following deposition of 100 cycles of La_2O_3 was unsuccessful (See Figure S1 in the Supplementary Materials.). Therefore, ALD growth rates were determined by measuring weight changes per cycle on 0.5-g samples of a γ-Al_2O_3 powder with a BET surface area of 130 m^2/g[17]. These data are shown in Figure 1 for each of the precursors. To calculate film thicknesses, the films were assumed to cover the γ-Al_2O_3 surface uniformly and have their bulk density. Previously published microscopy results on γ-Al_2O_3 suggest that the deposited films uniformly cover the surface of the γ-Al_2O_3 and have a thickness close to that calculated by the weight changes.[15,16] Based on these measurements, the growth rates were determined to be 0.024 nm ZrO_2/cycle, 0.019 nm La_2O_3/cycle, and 0.018 nm Fe_2O_3/cycle. To demonstrate that these growth rates are not strongly dependent on the substrate, measurements were also performed for Fe_2O_3 deposition on a 0.5-g sample of LSF powder with a surface area of 6 m^2/g. This showed a growth rate of 0.02 nm/cycle, a value essentially identical to that obtained on γ-Al_2O_3, but less accurate because of the lower surface area of the substrate. It is also worth noting that the growth rates for each of the oxides are similar to what is reported in some literature studies on nonporous substrates.[18,19]

$LaFeO_3$ films were grown by sequential deposition of La_2O_3 and Fe_2O_3, alternating between three cycles of La_2O_3 and one of Fe_2O_3 ALD cycle to ensure proper mixing of the stoichiometric amounts of each oxide. The 3:1 cycle ratio was calculated to give a 1:1 molar ratio of La and Fe based on the growth rates in Figure 1. To demonstrate that the perovskite structure could be formed, X-ray Diffraction (XRD) patterns were measured following deposition of a 1-nm film (45 cycles of La_2O_3 and 15 cycles of FeO_3) on γ-Al_2O_3. Figure 2 shows XRD patterns of the $LaFeO_3$/γ-Al_2O_3 after calcination at 873 and 1073 K, together with the unmodified γ-Al_2O_3. Peaks associated with the perovskite phase are clearly visible after heating to 873 K. These peaks show greatly increased intensity after heating to 1073 K; however, because $LaAlO_3$ has a nearly identical diffraction pattern as $LaFeO_3$ and could form at this higher temperature,[20] the pattern in Figure 2c could correspond to a mixture of $LaAlO_3$ and $LaFeO_3$.

The effect of modifying electrodes by ALD was studied on symmetric cells with LSF-YSZ composite electrodes similar to cells used in previous studies.[21,22] The electrolyte-supported cells were prepared by infiltration of aqueous solutions of La, Sr, and Fe salts ($La(NO_3)_3 \cdot 6H_2O$ (Alfa Aesar, 99.9%), $Sr(NO_3)_2$ (Alfa Aesar, 99%), and $Fe(NO_3)_3 \cdot 6H_2O$ (Fisher Scientific, 98.4%) in a molar ratio of La:Sr:Fe = 0.8:0.2:1) into the porous layers of porous-dense-porous, YSZ wafers. Citric acid, in a 1:1 ratio with the metal cations, was used as a complexing agent with the metal salts in order to assist the formation of the perovskite phase at the calcination temperature of 1123 K. The porous scaffolds were approximately 60% porous and had a pore structure similar to that of a sponge, with average pore sizes of approximately 2 μm. The electrodes were loaded to a level of 35-wt% LSF. The thickness of the dense and porous layers in the cells were 100 and 35 μm, respectively; and the effective surface area of the scaffolds was 0.35 cm^2.

After ALD modification, the cells were not heated above 873 K in most cases and electrode performance was characterized using

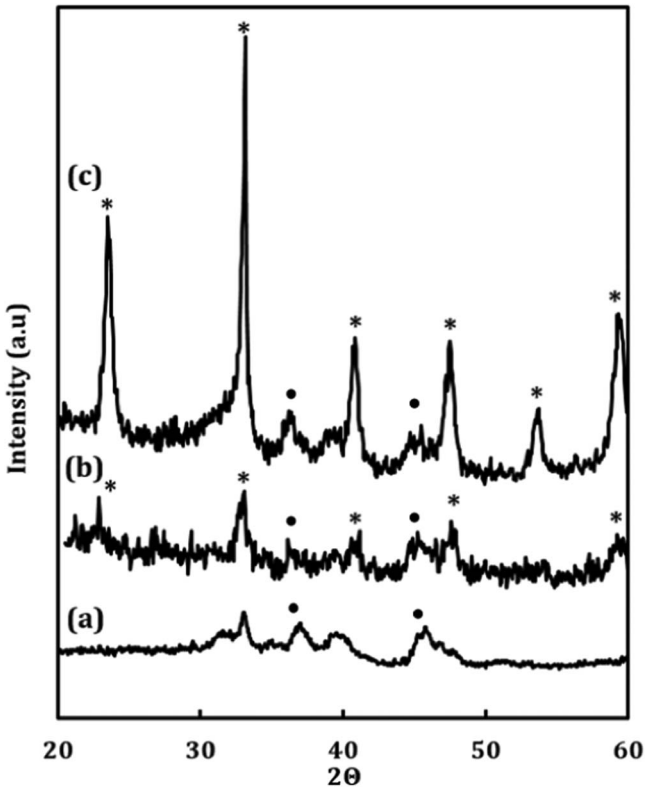

Figure 2. XRD patterns of the γ-Al_2O_3 sample before ALD modification and after depositing 45 ALD cycles La_2O_3 and 15 ALD cycles of Fe_2O_3. The XRD are of a) Fresh, unmodified γ-Al_2O_3; b) ALD-modified γ-Al_2O_3 after calcination to 873 K; c) the ALD-modified sample after calcination to 1073 K. Characteristic peaks for $LaFeO_3$ are marked by ∗, while obvious peaks associated with Al_2O_3 are marked by ●.

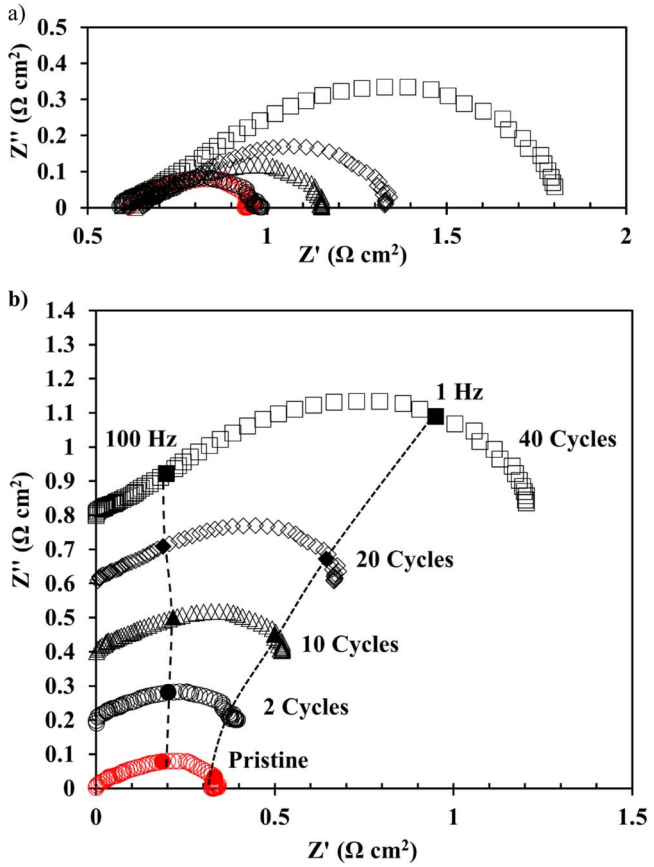

Figure 3. Impedance spectra for a symmetric cell with LSF-YSZ electrodes at 873 K after ZrO_2 ALD. Results are for reported for the pristine cell (◯) and after ZrO_2 ALD modification with 2 cycles (◯), 10 cycles (△), 20 cycles (◊), and 40 cycles (□). The spectra in a) and b) are the same except that the ohmic losses have been removed in b).

impedance spectroscopy at this temperature. This low temperature was chosen so as to avoid disrupting the ALD films. Silver paste was applied to each electrode for current collection; and impedance spectra were measured using a Gamry Instrument potentiometer, at open circuit, with a 1 mA AC perturbation. In order to achieve self-consistency in measuring the effect of each oxide film, a single cell was used for the entire series of measurements with that oxide. For example, in measuring the effects of ZrO_2 films on LSF-YSZ electrodes, impedance measurements were performed on the same cell, initially and after 0, 2, 10, 20, and 40 ALD cycles. In all cases, Ag paste was applied onto the electrodes just before electrochemical testing and removed carefully afterwards in order to perform subsequent ALD cycles. This allowed us to avoid the effects of any small variations between different cells. Null experiments were performed to ensure that the multiple steps involved in ALD – evacuation of the cell in the ALD system, removal of the Ag paste, and placement of the cell in the muffle furnace – had no effect on cell performance.

Results

To determine the effect ZrO_2 on the LSF-YSZ cathodes, impedance measurements were performed on symmetric cells after deposition of 0, 2, 10, 20, or 40 cycles by ALD. The samples were oxidized at 773 K after each deposition cycle; but the cells, at least at intermediate stages, were not heated to higher temperatures to avoid sintering of the film. For testing, the samples were simply ramped at 10 K/min to 873 K and impedance measurements were performed. The impedances, divided by two to account for the two electrodes, are shown in Figure 3. Spectra with the ohmic resistances included are given in Figure 3a; Figure 3b shows the same data with ohmic losses removed. As expected, the addition of ZrO_2 did not significantly affect the ohmic resistance. The ohmic resistance for each of the cells was 1.2 Ω cm^2 (2 × 0.6 Ω cm^2). The resistance for an 80-μm, YSZ electrolyte is expected to be between 1.1 and 1.3 Ω cm^2, using YSZ conductivities from the literature.[23]

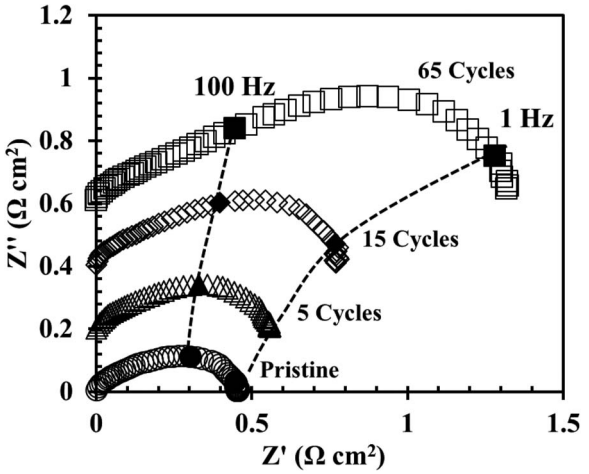

Figure 4. Impedance spectra for symmetric cells with LSF-YSZ electrodes at 873 K. Results are shown for the pristine cell (◯) and after ALD modification by Fe_2O_3 with 5 cycles (△), 15 cycles (◊), and 65 cycles (□).

By contrast, the effects of adding ZrO_2 on the non-ohmic losses at 873 K were significant. The non-ohmic losses in the pristine cell was 0.35 Ω cm^2, which is reasonably good cathode performance for a YSZ-based cell operating at this low temperature. The impedance increased in a regular manner with the addition of ZrO_2, to 0.4 Ω cm^2 after 2 ALD cycles and 0.52 Ω cm^2 after 10 cycles, then almost doubling to 0.7 Ω cm^2 after 20 ALD cycles and tripling to 1.2 Ω cm^2 after 40 cycles. It should be recognized that a growth rate of 0.024 nm/cycle corresponds to less than one monolayer per cycle and that each ZrO_2 species likely deposits in random positions each cycle. Also, if uniform, 20 and 40 ALD cycles would correspond to films that are only 0.5 and 1.0 nm thick, the equivalent of roughly 1 and 2 unit cells of cubic zirconia. Since previous work on essentially identical LSF-YSZ electrodes indicated that the performance of these cathodes is limited by O_2 adsorption,[21] the fact that such thin ZrO_2 films have a large effect implies that the ZrO_2 must be covering the surface uniformly and blocking the adsorption sites for O_2. It is also worth noting that the amount of ZrO_2 that was added to the electrodes was very small in all cases. Assuming that the specific surface area of the LSF-YSZ electrode was 2 m^2/g,[21] the weight of the electrode after 40 ALD cycles increases by only 1%.

Finally, to determine the thermal stability of the ZrO_2 films, the cell modified by 40 ALD cycles was heated to 973 K for 30 min and 1073 K for 1 min. This had no effect on impedance spectra measured at 873 K, demonstrating that at least the ZrO_2 films are reasonably stable.

Figure 4 shows the analogous results following ALD of Fe_2O_3 films on the LSF-YSZ electrodes at 873 K. The ohmic losses have been removed for clarity, since they did not change with the addition of Fe_2O_3. The initial non-ohmic impedance on this cell was 0.43 Ω cm^2 and this increased to 0.55 Ω cm^2 after 5 ALD cycles, 0.84 Ω cm^2 after 15 ALD cycles, and 1.32 Ω cm^2 after 65 ALD cycles. Since the growth rate for Fe_2O_3 was only 0.02 nm/cycle, the results again show that the Fe_2O_3 film must cover the surface uniformly. Given the similarity in the relationships between impedance and Fe_2O_3 and ZrO_2 film thickness, we suggest that both oxides increase impedance by simply blocking the surface and thereby limiting O_2 adsorption.

The results for LSF-YSZ cathode modification by La_2O_3 ALD, reported in Figure 5, exhibit some interesting differences from that observed for ZrO_2 and Fe_2O_3. When the electrode was treated with

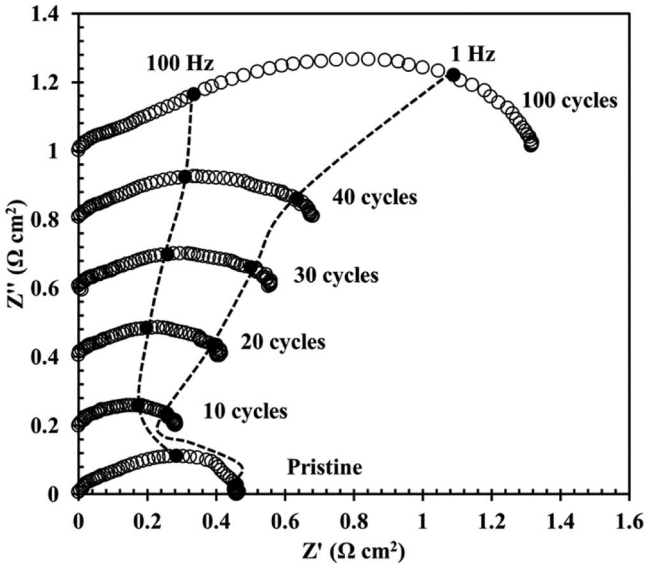

Figure 5. Impedance spectra for symmetric cells with LSF-YSZ electrodes at 873 K before and after the indicated number of La_2O_3 ALD cycles.

small numbers of ALD cycles, the impedance improved. This result was highly reproducible and achieved on multiple cells. For the particular cell used in taking the data in Figure 5, the polarization resistance dropped from an initial value of 0.46 Ω cm^2 to 0.28 Ω cm^2 after 10 La_2O_3 ALD cycles. Additional ALD cycles caused the non-ohmic impedance to increase. Starting from the cell with 20 ALD cycles, the deterioration in performance with increasing number of cycles is similar to that observed with ZrO_2 and Fe_2O_3, given that the growth rate for La_2O_3, 0.019 nm/cycle, was slightly lower.

Figure 6 shows results from experiments in which both La_2O_3 and Fe_2O_3 were deposited together. Results start from the bottom of the figure, with the effects of adding additional La_2O_3 and Fe_2O_3 proceeding upward. While we expected to achieve the best results when La and Fe were deposited in the perovskite stoichiometric ratio, the results were more complex and favored having excess La. Again, the results in Figure 6 were reproduced on multiple cells. First, the polarization resistance of the pristine LSF-YSZ cell at 873 K was 0.44 Ω cm^2; and the performance improved, to 0.28 Ω cm^2, following the addition of 3 ALD cycles of La_2O_3. Because the growth rate for Fe_2O_3 was three times that of La_2O_3 on an atomic basis, we then added 1 cycle of Fe_2O_3 to complete the perovskite lattice but this increased the impedance to 0.37 Ω cm^2. Subsequent addition of 3 more ALD cycles of La_2O_3 reduced the impedance to 0.27 Ω cm^2.

Since 7 ALD cycles, 6 La_2O_3 and 1 Fe_2O_3, corresponds to significantly less than a close-packed monolayer of the mixed oxide, the results to this point could be viewed as catalytic promotion of the initial LSF-YSZ electrode. To determine how a more complete overlayer would affect performance, we increased the coverages by a total of 15 La_2O_3 and 5 Fe_2O_3 cycles, alternating between 3 cycles of La_2O_3 for each cycle of Fe_2O_3. This increased the polarization resistance to 0.57 Ω cm^2. The subsequent addition of 3 more La_2O_3 cycles decreased this to 0.47 Ω cm^2. As a final experiment, we added 22 more cycles of La_2O_3 and 3 more of Fe_2O_3 in order to achieve a final film with a La:Fe stoichiometry of 5:3. The final polarization resistance was 0.37 Ω cm^2.

The results in Figure 6 demonstrate that, for thicker oxide coverages, having both La and Fe at the surface together improves the performance of the cell compared to what would be observed with the individual oxides. Having either 40 La_2O_3 ALD cycles or 8 Fe_2O_3 cycles would lead to significantly decreased performance compared to the pristine cell, while the cell with co-deposited La_2O_3 and Fe_2O_3 exhibited an impedance lower than that of the pristine cell. However, it does not appear that the best performance is achieved with the ideal

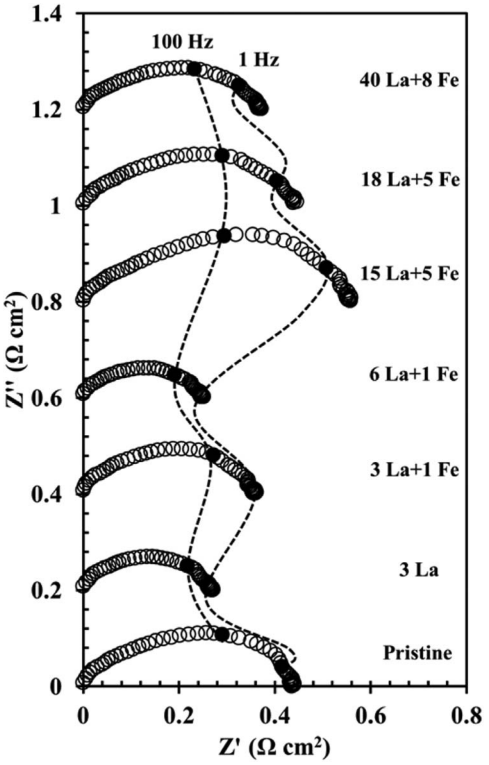

Figure 6. Impedance spectra for symmetric cells with LSF-YSZ electrodes at 873 K before and after sequential La_2O_3 and Fe_2O_3 ALD. The total number of ALD cycles is shown in the figure.

perovskite stoichiometry. All of the data following La_2O_3 and La_2O_3-Fe_2O_3 deposition suggest that having excess La near the surface is beneficial.

Discussion

The results of this study provide new insights into the use of ALD to modify the performance of SOFC cathodes. The fact that the impedance of infiltrated LSF-YSZ cathodes increased with an increased number of ALD cycles of ZrO_2 or Fe_2O_3 demonstrates that these oxides effectively block the oxygen adsorption/incorporation sites on the surface of the LSF. That the decrease in performance is severe for a total number of ALD cycles that produces films on the order of one nanometer thick also demonstrates that ALD can be used to deposit highly uniform layers on the surfaces of porous electrodes. Furthermore, the results obtained when alternating ALD cycles of La and Fe deposition demonstrate that the ALD method can be used to precisely grow uniform thin layers of perovskite oxides on cathode surfaces. This result is quite exciting because it provides for the possibility of optimizing the electrode performance through the use of mixed-oxide or perovskite layers with graded composition and/or through the growth of superlattices with two or more perovskite compositions.

The results for ALD deposition of La_2O_3 layers of the electrodes were more complex than those obtained for ZrO_2 or Fe_2O_3 and indicated that, for La_2O_3 ALD, there were at least two separate processes affecting the electrode performance. The increase in impedance at the higher La_2O_3 coverages can again simply be attributed to blocking of the surface oxygen adsorption sites by a thin, uniform film of La_2O_3. Since 100 ALD cycles corresponds to a film thickness of only 1.9 nm, the La_2O_3 layer appears to be very effective in blocking surface against O_2 adsorption. The more interesting process, however, occurs for less than 20 ALD cycles where the La_2O_3 coverage is less than or at most one monolayer. For these conditions, there is a noticeable

decrease in the electrode impedance relative to that in the pristine cell. Based solely on the data collected in the present study, we can only speculate as to the origin of this effect. It is noteworthy, however, that the effect is highly reproducible and leads to a significant enhancement in electrode performance. It is likely that, for these ALD conditions, the electrode surface is covered with isolated La_2O_3 clusters or scattered atoms. SOFC cathode performance is often thought to be limited by the oxygen-reduction reaction, which in turn can be suppressed by segregation of SrO to the surface in some cases. One possibility is that the enhanced performance upon addition of La_2O_3 is due to suppression of SrO segregation. That SrO segregation may be suppressed by modifying composition has recently been proposed.[32]

Comparison of the results of this study to those in previous literature studies also demonstrates that the properties of ALD-modified cathodes depend highly on the procedures and conditions used to carry out the ALD growth. As pointed out in the Introduction, two previous studies reported uniform deposition of porous ZrO_2 films in porous electrodes, with growth rates of roughly 0.6 nm/cycle.[4,5] In contrast, growth rates in our work were more than 20 times lower and the large effect of ALD modification on the electrode impedances in our work implies the films must be reasonably dense.

To explain the differences, it is worthwhile to consider that Keuter et al., using a precursor of similar size to that used in our studies, calculated the expected growth curves for ZrO_2 to be ~0.1 nm/cycle, based on the maximum surface density of precursor molecules which may adhere to the surface.[1] Furthermore, since chemical vapor deposition (CVD) would not produce uniform films in a porous substrate, it seems unlikely that CVD was important in any of the published work. The main difference between our homebuilt ALD apparatus and most commercial units is that, following exposure of the samples to the precursor molecules, the excess molecules in our system are removed by evacuation, rather than by flushing with an inert carrier gas. In porous materials, desorption rates are dramatically higher in vacuum compared to rates into a carrier gas.[24] Therefore, we suggest that at least some of the variability in the reported growth rates is related to how effectively excess precursor molecules are removed from the surface prior to the oxidation step in the cycle. Oxidation of a condensed layer of the precursors would lead to higher growth rates and films that are porous. There may be benefits to higher growth rates and porous films, but it is clearly important to have the ability to control the growth process.

There are important practical implications for using vacuum techniques in the performance of ALD. Gas-phase diffusion is very slow compared to Knudsen flow and deposition of uniform films on large-area electrochemical cells or powders is much more difficult in a flow system. It is for this reason that ALD on powders is often performed in a fluidized bed,[25] a procedure that is unnecessary if adsorption is performed on an evacuated sample. While the flow system allows better separation of the precursor and oxidizer for more rapid cycling, which is important for producing thicker films, the pore dimension in high-surface-area materials strongly limits how thick films can be, so that large numbers of cycles are not necessary.

While not fully explored in the present study, ALD can be a very important scientific tool for understanding the role that surface stoichiometry plays in electrode performance. Unlike infiltration procedures, ALD does not change the surface area of the electrode,[26] at least when conformal dense films are formed, so that performance can be more clearly linked to surface coverage. For example, deactivation in LSCF cathodes has frequently been associated with segregation of Sr cations.[27–29] The high degree of compositional control provided by ALD of Fe_2O_3 may allow titration of the Sr in the form of $SrFeO_3$ and re-activation of the electrode.[30,31]

Finally, we suggest that ALD has great promise for producing electrodes with complex and potentially promising surface structures. Here, we demonstrated that both pure and mixed-oxide films can be grown, but more complicated structures can be imagined. For example, there may be advantages to depositing multilayered structures. Obviously, the topic is still in its infancy.

Conclusions

1) The procedures used to grow oxide films in SOFC electrodes can affect film growth rates and morphology. ALD films grown using vacuum procedures form conformal, dense films on the electrode surface.
2) ZrO_2 and Fe_2O_3 films increase the polarization resistances of LSF-YSZ electrodes, apparently by covering O_2 adsorption sites.
3) Low coverages of La_2O_3 decrease the polarization resistance of LSF-YSZ electrodes but high coverages again increase the polarization resistance by blocking O_2 adsorption sites.
4) Low polarization resistances can be maintained for relatively thick oxide films when La_2O_3 and Fe_2O_3 are co-deposited. However, excess La_2O_3 must be present for the optimal stoichiometry.

Acknowledgments

This material is based upon work supported by the Department of Energy under Award Number DE-FE0023317. This report was prepared as an account of work sponsored by an agency of the United States Government. Neither the United States Government nor any agency thereof, nor any of their employees, makes any warranty, express or implied, or assumes any legal liability or responsibility for the accuracy, completeness, or usefulness of any information, apparatus, product, or process disclosed, or represents that its use would not infringe privately owned rights. Reference herein to any specific commercial product, process, or service by trade name, trademark, manufacturer, or otherwise does not necessarily constitute or imply its endorsement, recommendation, or favoring by the United States Government or any agency thereof. The views and opinions of authors expressed herein do not necessarily state or reflect those of the United States Government or any agency thereof.

References

1. T. Keuter, G. Mauer, F. Vondahlen, R. Iskandar, N. H. Menzler, and R. Vaßen, *Surf. Coat. Technol.*, **288**, 211 (2016).
2. A. Karimaghaloo, A. M. Andrade, S. Grewal, J. H. Shim, and M. H. Lee, *ACS Omega*, **2**(3), 806 (2017).
3. Y. Gong, D. Palacio, X. Song, R. L. Patel, X. Liang, X. Zhao, J. B. Goodenough, and K. Huang, *Nano Lett.*, **13**(9), 4340 (2013).
4. Y. Gong, R. L. Patel, X. Liang, D. Palacio, X. Song, J. B. Goodenough, and K. Huang, *Chem. Mater.*, **25**(21), 4224 (2013).
5. Y. Chen, K. Gerdes, and X. Song, *Sci. Rep.*, **6**(1) (2016).
6. H. J. Choi, K. Bae, D. Y. Jang, J. W. Kim, and J. H. Shim, *J. Electrochem. Soc.*, **162**(6), F622 (2015).
7. K.-Y. Liu, L. Fan, C.-C. Yu, and P.-C. Su, *Electrochem. Commun.*, **56**, 65 (2015).
8. K. C. Neoh, G. D. Han, M. Kim, J. W. Kim, H. J. Choi, S. W. Park, and J. H. Shim, *Nanotechnology*, **27**(18), 185403 (2016).
9. X. Cui, A. D. Zdunek, G. Jursich, and C. G. Takoudis, *ECS J. Solid State Sci. Technol.*, **4**(12), P429 (2015).
10. M. Cassir, A. Ringuedé, and L. Niinistö, *J. Mater. Chem.*, **20**(41), 8987 (2010).
11. M. Li, M. Zheng, B. Hu, Y. Zhang, and C. Xia, *Electrochimica Acta*, **230**, 196 (2017).
12. A. S. Yu, R. Küngas, J. M. Vohs, and R. J. Gorte, *J. Electrochem. Soc.*, **160**(11), F1225 (2013).
13. K. Yamahara, C. Jacobson, S. Visco, X. Zhang, and L. Dejonghe, *Solid State Ion.*, **176**(3–4), 275 (2005).
14. T. M. Onn, S. Zhang, L. Arroyo-Ramirez, Y.-C. Chung, G. W. Graham, X. Pan, and R. J. Gorte, *ACS Catal.*, **5**(10), 5696 (2015).
15. T. M. Onn, S. Zhang, L. Arroyo-Ramirez, Y. Xia, C. Wang, X. Pan, G. W. Graham, and R. J. Gorte, *Appl. Catal. B Environ.*, **201**, 430 (2017).
16. T. M. Onn, M. Monai, S. Dai, L. Arroyo-Ramirez, S. Zhang, X. Pan, G. W. Graham, P. Fornasiero, and R. J. Gorte, *Appl. Catal. A Gen.*, **534**, 70 (2017).
17. T. M. Onn, L. Arroyo-Ramirez, M. Monai, T.-S. Oh, M. Talati, P. Fornasiero, R. J. Gorte, and M. M. Khader, *Appl. Catal. B Environ.*, **197**, 280 (2016).
18. M. Putkonen and L. Niinistö, *J. Mater. Chem.*, **11**(12), 3141 (2001).
19. M. Rooth, A. Johansson, K. Kukli, J. Aarik, M. Boman, and A. Hårsta, *Chem. Vap. Depos.*, **14**(3), 67 (2008).
20. M. Ozawa, H. Toda, and S. Suzuki, *Appl. Catal. B Environ.*, **8**, 141 (1996).
21. R. Küngas, F. Bidrawn, E. Mahmoud, J. M. Vohs, and R. J. Gorte, *Solid State Ion.*, **225**, 146 (2012).
22. Y. Huang, J. M. Vohs, and R. J. Gorte, *J. Electrochem. Soc.*, **151**(4), A646 (2004).
23. V. Kharton, F. Marques, and A. Atkinson, *Solid State Ion.*, **174**(1–4), 135 (2004).
24. R. J. Gorte, *J. Catal.*, **75**, 164 (1982).
25. C.-L. Duan, P.-H. Zhu, Z. Deng, Y. Li, B. Shan, H.-S. Fang, G. Feng, and R. Chen, *J. Vac. Sci. Technol. Vac. Surf. Films*, **35**(1), 01B102 (2017).

26. F. Bidrawn, G. Kim, N. Aramrueang, J. M. Vohs, and R. J. Gorte, *J. Power Sources*, **195**(3), 720 (2010).
27. Y. Yu, K. F. Ludwig, J. C. Woicik, S. Gopalan, U. B. Pal, T. C. Kaspar, and S. N. Basu, *ACS Appl. Mater. Interfaces*, **8**(40), 26704 (2016).
28. J. Druce, H. Téllez, M. Burriel, M. D. Sharp, L. J. Fawcett, S. N. Cook, D. S. McPhail, T. Ishihara, H. H. Brongersma, and J. A. Kilner, *Energy Env. Sci*, **7**(11), 3593 (2014).
29. Y. Liu, K. Chen, L. Zhao, B. Chi, J. Pu, S. P. Jiang, and L. Jian, *Int. J. Hydrog. Energy*, **39**(28), 15868 (2014).
30. A. M. Ritzmann, J. M. Dieterich, and E. A. Carter, *MRS Commun.*, **6**(03), 145 (2016).
31. S. Jiang, J. Sunarso, W. Zhou, J. Shen, R. Ran, and Z. Shao, *J. Power Sources*, **298**, 209 (2015).
32. H. Kwon, W. Lee, and J. W. Han, *RSC Adv.*, **6**, 69782 (2016).